



## ORIGINAL ARTICLE

# Epigallocatechin Gallate-Mediated Alteration of the MicroRNA Expression Profile in 5 $\alpha$ -Dihydrotestosterone-Treated Human Dermal Papilla Cells

Shanghun Shin\*, Karam Kim\*, Myung Joo Lee, Jeongju Lee, Sungjin Choi, Kyung-Suk Kim, Jung-Min Ko, Hyunjoo Han, Su Young Kim, Hae Jeong Youn<sup>1</sup>, Kyu Joong Ahn<sup>1</sup>, In-Sook An<sup>2</sup>, Sungkwan An, Hwa Jun Cha

Korea Institute for Skin and Clinical Sciences and Molecular-Targeted Drug Research Center, Konkuk University, <sup>1</sup>Department of Dermatology, Konkuk University School of Medicine, Seoul, <sup>2</sup>KISCS Incorporated, Cheongju, Korea

**Background:** Dihydrotestosterone (DHT) induces androgenic alopecia by shortening the hair follicle growth phase, resulting in hair loss. We previously demonstrated how changes in the microRNA (miRNA) expression profile influenced DHT-mediated cell death, cell cycle arrest, cell viability, the generation of reactive oxygen species (ROS), and senescence. Protective effects against DHT have not, however, been elucidated at the genome level. **Objective:** We showed that epigallocatechin gallate (EGCG), a major component of green tea, protects DHT-induced cell death by regulating the cellular miRNA expression profile. **Methods:** We used a miRNA microarray to identify miRNA expression levels in human dermal papilla cells (DPCs). We investigated whether the miRNA expression influenced the protective effects of EGCG against DHT-induced cell death, growth arrest, intracellular ROS levels, and senescence. **Results:** EGCG protected against the effects of DHT by altering the miRNA expression profile in human DPCs. In addition, EGCG attenuated DHT-mediated cell death and growth ar-

rest and decreased intracellular ROS levels and senescence. A bioinformatics analysis elucidated the relationship between the altered miRNA expression and EGCG-mediated protective effects against DHT. **Conclusion:** Overall, our results suggest that EGCG ameliorates the negative effects of DHT by altering the miRNA expression profile in human DPCs. (*Ann Dermatol* 28(3) 327~334, 2016)

**-Keywords-**

Epigallocatechin gallate, Human dermal papilla cells, MicroRNAs

## INTRODUCTION

Androgenic alopecia causes hair loss by shortening the growth phase (anagen) of hair follicles; it is provoked by excessive androgen-receptor activation by androgens such as testosterone and dihydrotestosterone (DHT) in post-pubertal males<sup>1-3</sup>. Androgen-induced regulation of the hair growth cycle results in early growth cessation (catagen)<sup>4</sup>. Specifically, DHT produced by 5 $\alpha$ -reductase strongly activates the androgen receptors, because its binding affinity is two to three times that of testosterone<sup>5,6</sup>. The activity or expression of 5 $\alpha$ -reductase is elevated in most cases of androgenic alopecia<sup>7</sup>. Therefore, 5 $\alpha$ -reductase and androgen receptors are attractive therapeutic targets for that condition<sup>8,9</sup>. The DHT-mediated activation of androgen receptors induces the expression of various downstream genes that are related to hair follicle development, morphology, and cell cycling<sup>10,11</sup>.

In a recent study, DHT was shown to regulate microRNAs

Received June 8, 2015, Revised August 4, 2015, Accepted for publication August 11, 2015

\*These authors contributed equally to this work.

**Corresponding author:** Hwa Jun Cha, Korea Institute for Skin and Clinical Sciences and Molecular-Targeted Drug Research Center, Konkuk University, 120 Neungdong-ro, Gwangjin-gu, Seoul 05029, Korea. Tel: 82-2-450-3743, Fax: 82-2-3437-8360, E-mail: hjcha@konkuk.ac.kr

This is an Open Access article distributed under the terms of the Creative Commons Attribution Non-Commercial License (<http://creativecommons.org/licenses/by-nc/4.0>) which permits unrestricted non-commercial use, distribution, and reproduction in any medium, provided the original work is properly cited.

Copyright © The Korean Dermatological Association and The Korean Society for Investigative Dermatology

(miRNAs) in dermal papilla cells (DPCs), a group of specialized fibroblasts within the hair follicle bulb<sup>12</sup>. Additionally, miRNAs exhibit altered expression profiles in the balding dermal papilla<sup>13</sup>. miRNAs are small, non-coding RNAs containing 19~24 nucleotides. They target specific sequences within messenger RNAs (mRNAs) and repress mRNA translation, thus playing important roles in the development, cell cycle regulation, apoptosis, differentiation, and cell proliferation<sup>12-14</sup>.

Epigallocatechin gallate (EGCG), a representative ingredient in green tea, is a major polyphenolic constituent used widely for its anti-cancer effects, protection against ultraviolet light-induced DNA damage, and antioxidant and anti-inflammation activities<sup>15-20</sup>. In hair follicles, EGCG prevents androgenic alopecia by inhibiting 5 $\alpha$ -reductase activity<sup>21</sup>. EGCG promotes hair growth by activating Erk and Akt signaling and increasing the B-cell lymphoma 2 (BCL2)/Bax ratio in DPCs<sup>22</sup>. Additionally, it has been reported that EGCG protects against ultraviolet light-mediated cell death and cell cycle arrest by regulating specific miRNAs<sup>23</sup>. Here, we demonstrate that EGCG protects against DHT-induced cell death, cell cycle arrest, senescence, and oxidative stress in human DPCs by inducing changes in the miRNA expression profile.

## MATERIALS AND METHODS

### Chemicals and cell culture

EGCG and DHT were purchased from Sigma-Aldrich (St. Louis, MO, USA). Human DPCs (Innoprot, Biscay, Spain), characterized and isolated from the frontal head region of a non-balding male 34 years of age, were maintained in Dulbecco's minimal essential medium (DMEM; Gibco/Life Technologies, Carlsbad, CA, USA) supplemented with 10% fetal bovine serum (Sigma-Aldrich), 100 IU/ml penicillin, and 100  $\mu$ g/ml streptomycin. The cultures were incubated at 37°C in a humidified atmosphere of 5% CO<sub>2</sub>.

### Cell viability assay

Human DPCs were seeded in 96-well plates (5 $\times$ 10<sup>3</sup> cells per well) in triplicate. After 24 hours, the cells were exposed to the indicated concentrations of DHT and EGCG. To assess the cell viability, the cells were incubated in a water soluble tetrazolium salt (WST-1) solution for 30 minutes, and the optical density at 490 nm was subsequently measured.

### Cell cycle analysis

Human DPCs (2 $\times$ 10<sup>6</sup> cells) were seeded in 60 mm culture dishes and cultured for 24 hours in DMEM. The cells were then treated with DHT and EGCG for 24 hours.

Then, the cells were digested with 0.25% trypsin (Gibco/Life Technologies), fixed with 70% ethanol for 3 hours, and stained with propidium iodide (PI; Sigma-Aldrich). After 1 hour incubation, the cells were washed with phosphate-buffered saline, and a FACSCaliber flow cytometer (BD Biosciences, San Jose, CA, USA) was used to analyze their fluorescence intensity in the FL2 channel (excitation wavelength, 488 nm; emission wavelength, 578 nm).

### Intracellular reactive oxygen species analysis

Human DPCs (2 $\times$ 10<sup>6</sup> cells) were seeded in 60 mm culture dishes and cultured for 24 hours in DMEM. They were then treated with DHT and EGCG as indicated for 24 hours. Next, 20  $\mu$ M 2',7'-dichlorofluorescein diacetate (Sigma-Aldrich) was added to the culture medium for 1 hour. The cells were then digested with 0.25% trypsin and washed with phosphate-buffered saline. The stained cells were analyzed using a FACSCaliber flow cytometer (BD Biosciences) with the FL1 channel (excitation wavelength, 488 nm; emission wavelength, 530 nm).

### Cell senescence analysis

Human DPCs (2 $\times$ 10<sup>6</sup> cells) were seeded in 60 mm culture dishes and cultured for 24 hours in DMEM. They were then treated with DHT and EGCG as indicated for 48 hours. Next, the cells were fixed and stained with a senescence detection kit (Biovision, Milpitas, CA, USA) and observed under a light microscope (Olympus DSU, Tokyo, Japan).

### Total RNA extraction and miRNA expression profile

Total cellular RNA was isolated with TRIzol reagent (Invitrogen/Life Technologies, Grand Island, NY, USA) according to the manufacturer's instructions. miRNA labeling, hybridization, and microarray analyses were performed as described previously<sup>24</sup>. The isolated RNAs were labeled with Cy3 using the Agilent miRNA labeling kit (Agilent Technologies, Santa Clara, CA, USA). The labeled RNAs were purified using Micro Bio-Spin P-6 columns (Bio-Rad Laboratories, Hercules, CA, USA). For the miRNA expression profile, the SurePrint G3 Human V16 miRNA 8 $\times$ 60 K array (Agilent Technologies), including 1205 annotated miRNA sequences, was hybridized with the labeled total cellular RNA at 65°C for 20 hours. The microarray was scanned using an Agilent Microarray Scanner (Agilent Technologies), and the images were analyzed using the Agilent Feature Extraction Software (Agilent Technologies). A signal analysis of the microarrays (GeneSpring GX ver. 11.5, Agilent Technologies) compared the fluorescence intensities between samples obtained from control and EGCG-treated human DPCs,

respectively.

### Bioinformatics analysis and target prediction

The PITA (<http://genie.weizmann.ac.il>), microRNAorg (<http://www.microRNA.org>), and TargetScan (<http://www.targetscan.org>) online software programs were used for bioinformatics analysis and miRNA target prediction. The gene ontologies (GOs) of the putative target genes were analyzed using the Database for Annotation, Visualization, and Integrated Discovery Bioinformatics Resource 6.7 (<http://david.abcc.ncifcrf.gov>).

### Statistical analysis

The data are presented as the mean  $\pm$  standard deviation. Statistical significance was calculated using Student's two-tailed t-test, and  $p < 0.01$  was considered statistically significant unless otherwise indicated.

## RESULTS

### EGCG attenuated DHT-induced growth arrest in human DPCs

To determine the effect of EGCG on the cytotoxicity of DHT in human DPCs, we performed cell viability assays.

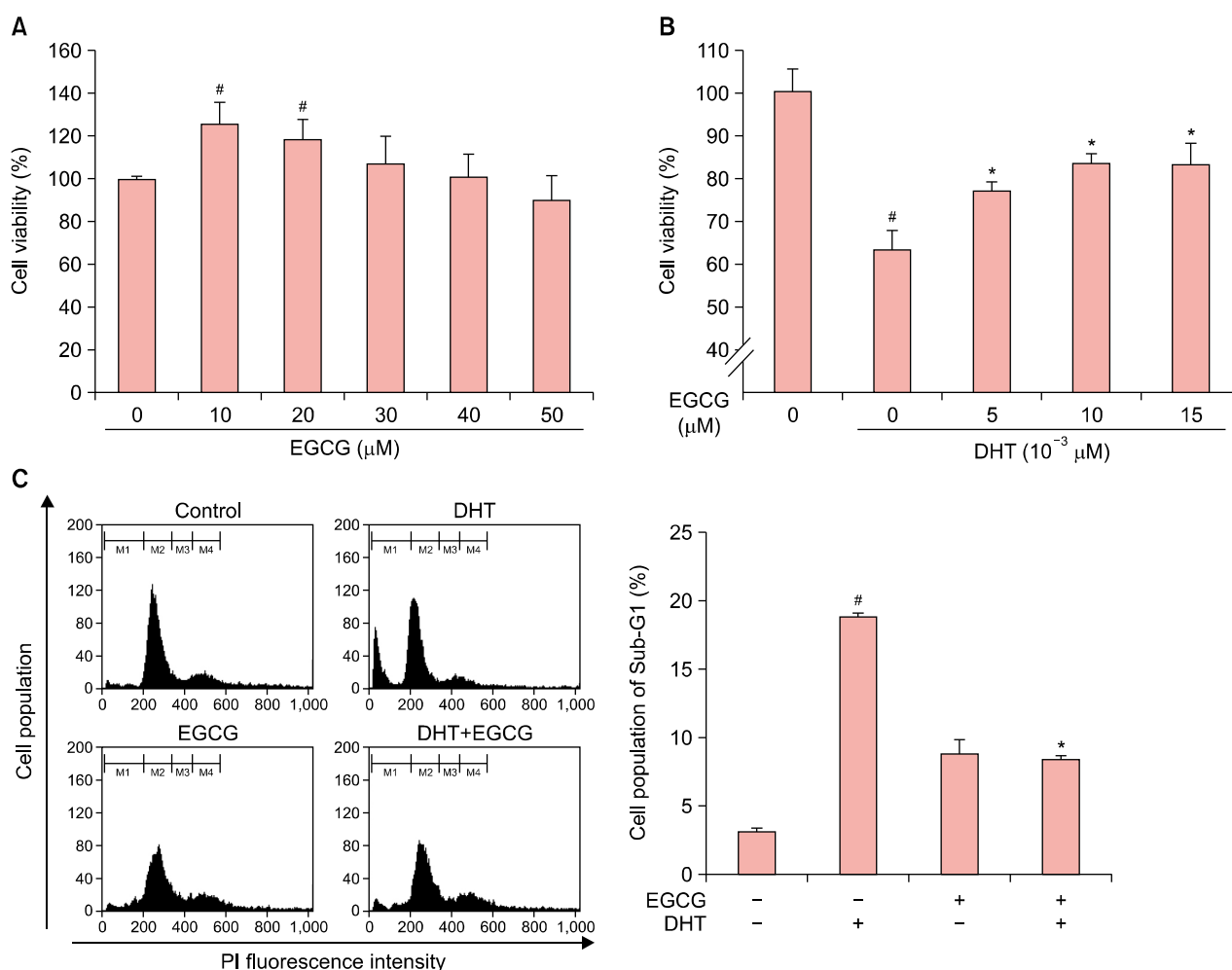


**Fig. 1.** Effects of epigallocatechin gallate (EGCG) on human dermal papilla cell (DPC) viability and cell cycle progression. Human DPCs were treated with different concentrations of EGCG (A) or EGCG and dihydrotestosterone (DHT) (B) for 24 hours before water soluble tetrazolium salt (WST-1) assays to measure viability. (C) Human DPCs were treated with 10  $\mu\text{M}$  EGCG or  $10^{-4}$  M DHT for 24 hours before they were washed and stained with propidium iodide (PI; Sigma-Aldrich, St. Louis, MO, USA). The fluorescence intensity distributions of the stained cells were analyzed by flow cytometry (left) and the proportions of the cells in Sub-G1 phase were determined (right). Cells in the Sub-G1, G1, S, and G2/M phases were separated using the gates M1, M2, M3, and M4, respectively. Viability data are expressed as percentages of the viability of the internal control (untreated sample) and are shown as the mean  $\pm$  standard error of the mean of three independent experiments. <sup>#</sup> $p < 0.05$  compared with vehicle, <sup>\*</sup> $p < 0.05$  compared with DHT.

The cell viability increased with 10  $\mu$ M EGCG, but it decreased with EGCG concentrations  $\geq 20$   $\mu$ M (Fig. 1A). That result corroborates a previous finding that EGCG has concentration-dependent dual functions<sup>25</sup>. Next, we investigated whether EGCG protected against DHT-induced growth arrest. EGCG (0~15  $\mu$ M) attenuated DHT-induced growth arrest in the human DPCs in a dose-dependent manner (Fig. 1B). All three of the EGCG doses tested produced significant protective effects. In addition, EGCG decreased levels of DHT-mediated cell death (Fig. 1C). Overall, DHT decreased cell viability, but the EGCG treatments rescued the DHT-mediated decrease in cell viability by repressing cell death.

### EGCG ameliorated DHT-induced reactive oxygen species levels and senescence in human DPCs

EGCG ameliorated the DHT-mediated elevation of intracellular reactive oxygen species (ROS) levels (Fig. 2A). Because intracellular ROSs are involved in inducing senescence<sup>11</sup>, we investigated whether EGCG inhibited senescence in human DPCs by quantifying the activity of senescence-associated  $\beta$ -gal. As shown in Fig. 2B, EGCG significantly inhibited DHT-induced senescence.

escence-associated  $\beta$ -gal. As shown in Fig. 2B, EGCG significantly inhibited DHT-induced senescence.

### EGCG altered miRNA expression profiles in DHT-treated human DPCs

Finally, we assessed whether EGCG altered miRNA expression profiles in DHT-treated human DPCs. Recent studies have shown that EGCG is a natural regulator of miRNAs that can influence cell growth, apoptosis, and cell cycle regulation. Among the 1205 annotated miRNAs analyzed, 13 miRNAs showed up-regulation by more than twofold, and 40 miRNAs showed down-regulation by more than twofold after EGCG administration to DHT-treated human DPCs (Table 1).

Using three bioinformatics and target prediction systems, we identified target genes of 54 miRNAs that were up-regulated or down-regulated by the EGCG treatment in DHT-treated human DPCs (Table 2). Overall, we analyzed 306 putative target genes of 13 up-regulated miRNAs and 134 putative target genes of 40 down-regulated miRNAs. Next, we identified the biological roles of the putative target

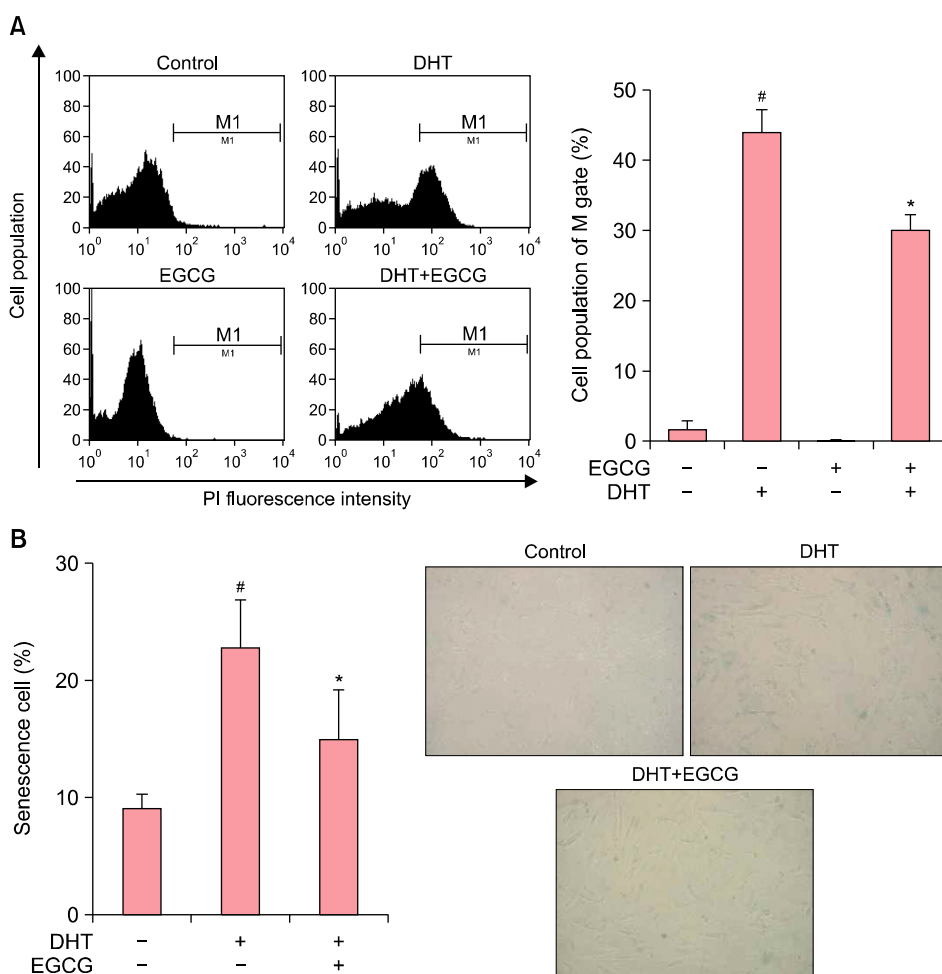


**Fig. 2.** Effects of epigallocatechin gallate (EGCG) on intracellular reactive oxygen species (ROS) levels and cellular senescence in human dermal papilla cells (DPCs). (A) Human DPCs were grown with or without 10  $\mu$ M EGCG and 10<sup>-4</sup> M dihydrotestosterone (DHT). To detect intracellular ROS levels, we performed 2',7'-dichlorofluorescein diacetate staining and detected cell cycle changes using a FACScalibur flow cytometer (BD Biosciences, San Jose, CA, USA). Changes in intracellular ROS levels were determined with the M1 gate. (B) Cells were treated with 10  $\mu$ M EGCG or 10<sup>-4</sup> M DHT for 48 hours. Senescence was measured using senescence-associated  $\beta$ -gal assays. Senescence data are expressed as percentages of the senescence of the internal control (untreated sample) and are shown as the mean  $\pm$  standard error of the mean of three independent experiments. PI: propidium iodide (Sigma-Aldrich, St. Louis, MO, USA). <sup>#</sup>*p* < 0.05 compared with vehicle, <sup>\*</sup>*p* < 0.05 compared with DHT.

**Table 1.** miRNAs from hDPCs with >2 fold expression change following EGCG and DHT treatment

miRNA	Fold change	Direction of change to control	Chr	miRNA	Fold change	Direction of change to control	Chr
hsa-miR-181b	2.17	Up	chr1	hsa-miR-17*	-82.18	Down	chr13
hsa-miR-181d	137.76	Up	chr19	hsa-miR-1825	-126.92	Down	chr20
hsa-miR-210	330.95	Up	chr11	hsa-miR-186	-61.81	Down	chr1
hsa-miR-3656	2.26	Up	chr11	hsa-miR-188-5p	-147.60	Down	chrX
hsa-miR-370	2.22	Up	chr14	hsa-miR-18b*	-56.14	Down	chrX
hsa-miR-4257	66.47	Up	chr1	hsa-miR-202	-47.66	Down	chr10
hsa-miR-4270	2.88	Up	chr3	hsa-miR-204	-55.37	Down	chr9
hsa-miR-4271	2.17	Up	chr3	hsa-miR-28-5p	-49.61	Down	chr3
hsa-miR-4327	4.05	Up	chr21	hsa-miR-3180-5p	-53.64	Down	chr16
hsa-miR-590-5p	147.55	Up	chr7	hsa-miR-324-5p	-49.46	Down	chr17
hsa-miR-629*	140.42	Up	chr15	hsa-miR-33b*	-26.10	Down	chr17
hsa-miR-718	104.88	Up	chrX	hsa-miR-3613-3p	-106.25	Down	chr13
hsa-miR-762	2.12	Up	chr16	hsa-miR-3676	-135.08	Down	chr17
hsa-let-7a*	-38.70	Down	chr9	hsa-miR-369-3p	-49.41	Down	chr14
hsa-miR-100*	-51.87	Down	chr11	hsa-miR-3907	-2.66	Down	chr7
hsa-miR-1225-3p	-2.00	Down	chr16	hsa-miR-411*	-29.26	Down	chr14
hsa-miR-1249	-48.55	Down	chr22	hsa-miR-425*	-125.74	Down	chr3
hsa-miR-128	-48.31	Down	chr2	hsa-miR-4306	-121.68	Down	chr13
hsa-miR-1281	-104.56	Down	chr22	hsa-miR-431	-48.51	Down	chr14
hsa-miR-129-3p	-58.90	Down	chr11	hsa-miR-431*	-34.81	Down	chr14
hsa-miR-136	-2.09	Down	chr14	hsa-miR-4317	-52.71	Down	chr18
hsa-miR-138-2*	-71.90	Down	chr16	hsa-miR-550a	-25.75	Down	chr7
hsa-miR-146a	-49.51	Down	chr5	hsa-miR-664	-140.38	Down	chr1
hsa-miR-150*	-54.57	Down	chr19	hsa-miR-766	-2.38	Down	chrX
hsa-miR-1539	-55.61	Down	chr18	hsa-miR-770-5p	-77.43	Down	chr14
hsa-miR-16-2*	-26.03	Down	chr3	hsa-miR-933	-31.12	Down	chr2

miRNA: microRNA, hDPC: human dermal papillary cell, EGCG: epigallocatechin gallate, DHT: dihydrotestosterone, chr: chromosome.

**Table 2.** Number of targets of selected miRNAs based on three prediction databases

Targets of up-regulated miRNAs			Targets of down-regulated miRNAs		
Targetscan	PITA	microRNAorg	Targetscan	PITA	microRNAorg
673	415	833	535	173	470
Intersection of three target prediction databases: 306			Intersection of three target prediction databases: 134		

TargetScan: <http://www.targetscan.org>, PITA: <http://genie.weizmann.ac.il>, microRNAorg: <http://www.microrna.org>, miRNAs: microRNAs.

genes by GO analysis. The putative target genes were classified into five major functional categories: anti-oxidation, apoptosis and cell death, proliferation and cell growth, aging, and cell cycle-related (Fig. 3). The protective effects of EGCG against DHT-mediated growth arrest, cell death, increased ROS, and senescence were strongly associated with the altered miRNA expression profile.

## DISCUSSION

In the present study, we showed the biological effects of EGCG and EGCG-mediated changes in miRNA profiles in DHT-exposed human DPCs. EGCG is a well-known, du-

al-role agent that protects against cellular damage in impaired cells and also induces cell death in various tumors<sup>26-31</sup>. We investigated whether EGCG reduced DHT-mediated cellular damage in human DPCs. The results shown in Figs. 1 and 2 suggest that EGCG inhibits DHT-induced cell death, intracellular ROS levels, and senescence. In general, DHT increases intracellular ROS levels, which induce cell death and growth arrest<sup>32,33</sup>. EGCG, a powerful antioxidant, ameliorated the DHT-mediated elevation of intracellular ROS levels and thus protected the human DPCs<sup>17</sup>. EGCG treatment alone slightly increased the sub-G1 cell population, however, which suggests that EGCG induced some cell death under

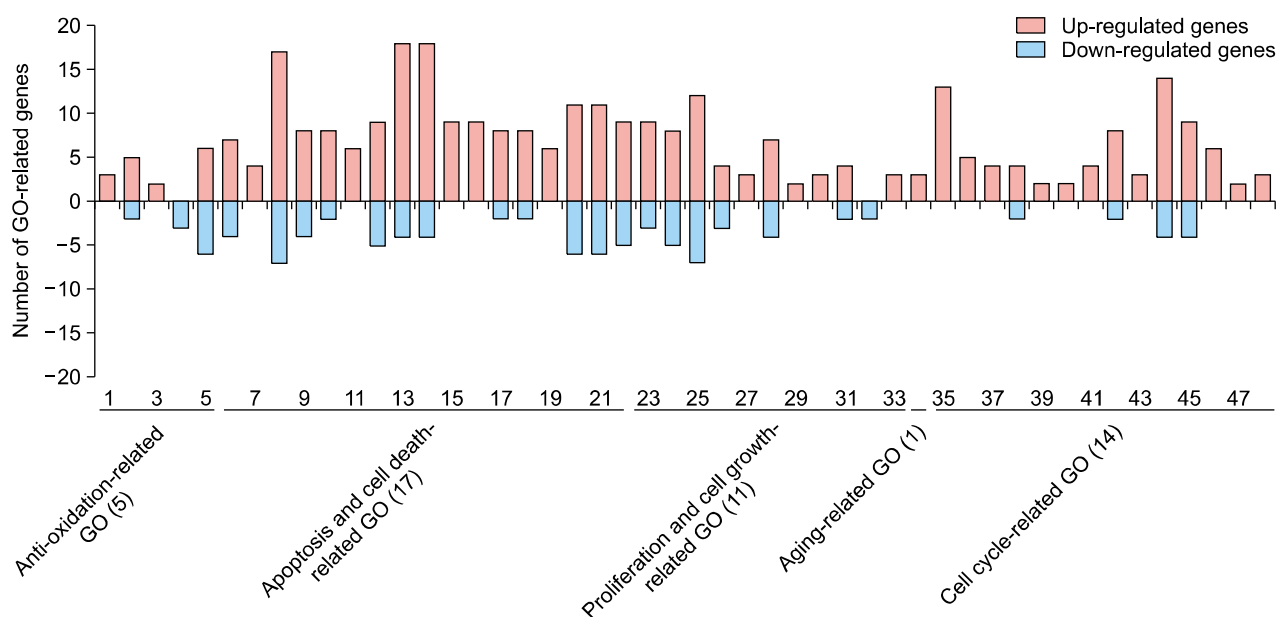


**Fig. 3.** Gene ontology classification of predicted target genes of microRNAs affected by epigallocatechin gallate in dihydrotestosterone-treated human dermal papilla cells. GO terms 1~5 are related to anti-oxidation: 1-oxidoreduction coenzyme metabolic process (GO:0006733); 2-response to oxidative stress (GO:0006979); 3-response to hydrogen peroxide (GO:0042542); 4-energy derivation by oxidation of organic compounds (GO:0015980); 5-oxidation reduction (GO:0055114). GO terms 6~22 are related to apoptosis and cell death: 6-anti-apoptosis (GO:0006916); 7-induction of apoptosis by extracellular signals (GO:0008624); 8-regulation of apoptosis (GO:0042981); 9-negative regulation of apoptosis (GO:0043066); 10-positive regulation of apoptosis (GO:0043065); 11-induction of apoptosis (GO:0006917); 12-apoptosis (GO:0006915); 13-regulation of programmed cell death (GO:0043067); 14-regulation of cell death (GO:0010941); 15-negative regulation of programmed cell death (GO:0043069); 16-negative regulation of cell death (GO:0060548); 17-positive regulation of programmed cell death (GO:0043068); 18-positive regulation of cell death (GO:0010942); 19-induction of programmed cell death (GO:0012502); 20-cell death (GO:0008219); 21-death (GO:0016265); 22-programmed cell death (GO:0012501). GO terms 23~33 are related to proliferation and cell growth: 23-cell proliferation (GO:0008283); 24-positive regulation of cell proliferation (GO:0008284); 25-regulation of cell proliferation (GO:0042127); 26-negative regulation of cell proliferation (GO:0008285); 27-negative regulation of cell growth (GO:0030308); 28-regulation of growth (GO:0040008); 29-regulation of developmental growth (GO:0048638); 30-negative regulation of growth (GO:0045926); 31-regulation of cell growth (GO:0001558); 32-positive regulation of growth (GO:0045927); 33-growth (GO:0040007). GO term 34 is related to aging (34-aging (GO:0007568). GO terms 35~48 are related to the cell cycle: 35-regulation of cell cycle (GO:0051726); 36-negative regulation of cell cycle (GO:0045786); 37-M phase of meiotic cell cycle (GO:0051327); 38-meiotic cell cycle (GO:0051321); 39-negative regulation of mitotic cell cycle (GO:0045930); 40-negative regulation of cell cycle process (GO:0010948); 41-regulation of mitotic cell cycle (GO:0007346); 42-cell cycle phase (GO:0022403); 43-regulation of cell cycle process (GO:0010564); 44-cell cycle (GO:0007049); 45-cell cycle process (GO:0022402); 46-mitotic cell cycle (GO:0000278); 47-cell cycle checkpoint (GO:0000075); 48-M phase of mitotic cell cycle (GO:0000087).

normal conditions (Fig. 1C). Several previous studies have shown that high concentrations of EGCG induce cell death and cell cycle arrest in various cancers<sup>28-31</sup>. Lu et al.<sup>34</sup> showed that EGCG can induce cell death at low concentrations (< 100  $\mu$ M) in normal human lung and skin cells, because antioxidants such as EGCG eliminate intercellular ROSs used as signal molecules<sup>34,35</sup>. Thus, low concentrations of EGCG can induce some degree of cell death under normal conditions.

We showed the effects of EGCG on the miRNA profile in DHT-exposed human DPCs. EGCG significantly up-regulated or down-regulated 53 miRNAs. Previous studies have identified direct target genes and physiological roles

in some of those miRNAs. Hsa-miR-210 (330.95-fold increase) promotes proliferation and represses growth arrest through the targeting of fibroblast growth factor receptor-like 1 (FGFRL1), apoptosis-inducing factor, mitochondrion-associated 3 (AIFM3), stathmin (STMN1), probable dimethyladenosine transferase (DIMT1), protein tyrosine phosphatase non-receptor type 2 (PTPN2), and iron-sulfur cluster scaffold homolog 2 (ISCU2)<sup>36-39</sup>. Hsa-miR-590-5p (147.55-fold increase) promotes cell growth and survival by targeting the S100 calcium-binding protein A10 (S100A10), transforming growth factor beta receptor II (TGF- $\beta$  RII), and close homolog of L1 (CHL1)<sup>40-42</sup>. The overexpression of hsa-miR-370 (2.22-fold increase) in-

duces proliferation by interfering with forkhead box protein O1 (FOXO1)<sup>43,44</sup>. Hsa-miR-188-5p (147.60-fold decrease) suppresses the G1/S transition by targeting cyclin D1 (CCND1), CCND3, CCNE2, CCNA2, cyclin-dependent kinase 4 (CDK4), and CDK2<sup>45</sup>. Hsa-miR-28-5p (49.61-fold decrease) targets MAD2 mitotic arrest deficient-like 1 (MAD2L1), BCL2-associated athanogene (BAG1), and the rat sarcoma viral oncogene homolog (RAS) oncogene family (RAP1B and RAB23)<sup>46</sup>, which can regulate cell proliferation, migration, and invasion by influencing spindle checkpoint control, apoptosis, and GTPase-mediated signal transduction.

Furthermore, we predicted the targets of a number of the EGCG-regulated miRNAs using Targetscan, PITA, and microRNAorg (Table 2). Many of the predicted target genes are associated with pathways regulating anti-oxidation, apoptosis and cell death, proliferation and cell growth, aging, and the cell cycle (Fig. 3). Our results show that the EGCG-mediated regulation of those regulatory pathways is related to alterations of miRNA expression in DHT-exposed human DPCs.

Overall, our investigation revealed EGCG-mediated changes in miRNA expression that protect against the DHT-induced human DPC phenotype. Our microarray analyses show that EGCG modulates the expression of miRNAs involved in oxidation, apoptosis and cell death, proliferation and cell growth, aging, and the cell cycle, providing an overall protective effect against DHT.

## ACKNOWLEDGMENT

This study was supported by the KU Research Professor (H. J. Cha) Program of Konkuk University. This study was also supported by a grant from the Ministry of Science, ICT and Future Planning (no. 20110028646) of the Republic of Korea and a grant from the Korean Health Technology R&D Project, Ministry of Health & Welfare, Republic of Korea (grant no. HN13C0075).

## REFERENCES

1. Van Neste D, Fuh V, Sanchez-Pedreno P, Lopez-Bran E, Wolff H, Whiting D, et al. Finasteride increases anagen hair in men with androgenetic alopecia. *Br J Dermatol* 2000; 143: 804-810.
2. Trüeb RM. Molecular mechanisms of androgenetic alopecia. *Exp Gerontol* 2002;37:981-990.
3. Lee WS, Lee HJ. Characteristics of androgenetic alopecia in asian. *Ann Dermatol* 2012;24:243-252.
4. Hibino T, Nishiyama T. Role of TGF-beta2 in the human hair cycle. *J Dermatol Sci* 2004;35:9-18.
5. Randall VA. Role of 5 alpha-reductase in health and disease. *Baillieres Clin Endocrinol Metab* 1994;8:405-431.
6. Horton R, Pasupuletti V, Antonipillai I. Androgen induction of steroid 5 alpha-reductase may be mediated via insulin-like growth factor-I. *Endocrinology* 1993;133:447-451.
7. Reborna A. Pathogenesis of androgenetic alopecia. *J Am Acad Dermatol* 2004;50:777-779.
8. Ellis JA, Sinclair R, Harrap SB. Androgenetic alopecia: pathogenesis and potential for therapy. *Expert Rev Mol Med* 2002;4:1-11.
9. Jain R, De-Eknamkul W. Potential targets in the discovery of new hair growth promoters for androgenic alopecia. *Expert Opin Ther Targets* 2014;18:787-806.
10. Kamik P, Shah S, Dvorkin-Wininger Y, Oshtory S, Mirmirani P. Microarray analysis of androgenetic and senescent alopecia: comparison of gene expression shows two distinct profiles. *J Dermatol Sci* 2013;72:183-186.
11. Lai JJ, Chang P, Lai KP, Chen L, Chang C. The role of androgen and androgen receptor in skin-related disorders. *Arch Dermatol Res* 2012;304:499-510.
12. Lee MJ, Cha HJ, Lim KM, Lee OK, Bae S, Kim CH, et al. Analysis of the microRNA expression profile of normal human dermal papilla cells treated with 5  $\alpha$ -dihydrotestosterone. *Mol Med Rep* 2015;12:1205-1212.
13. Goodarzi HR, Abbasi A, Saffari M, Fazelzadeh Haghghi M, Tabei MB, Noori Dalooi MR. Differential expression analysis of balding and nonbalding dermal papilla microRNAs in male pattern baldness with a microRNA amplification profiling method. *Br J Dermatol* 2012;166:1010-1016.
14. Cha HJ, Kim OY, Lee GT, Lee KS, Lee JH, Park IC, et al. Identification of ultraviolet B radiation-induced microRNAs in normal human dermal papilla cells. *Mol Med Rep* 2014; 10:1663-1670.
15. Lecumberri E, Dupertuis YM, Miralbell R, Pichard C. Green tea polyphenol epigallocatechin-3-gallate (EGCG) as adjuvant in cancer therapy. *Clin Nutr* 2013;32:894-903.
16. Shankar S, Ganapathy S, Srivastava RK. Green tea polyphenols: biology and therapeutic implications in cancer. *Front Biosci* 2007;12:4881-4899.
17. Du GJ, Zhang Z, Wen XD, Yu C, Calway T, Yuan CS, et al. Epigallocatechin Gallate (EGCG) is the most effective cancer chemopreventive polyphenol in green tea. *Nutrients* 2012;4:1679-1691.
18. Muthusamy V, Piva TJ. The UV response of the skin: a review of the MAPK, NFkappaB and TNFalpha signal transduction pathways. *Arch Dermatol Res* 2010;302:5-17.
19. Zhu W, Xu J, Ge Y, Cao H, Ge X, Luo J, et al. Epigallocatechin-3-gallate (EGCG) protects skin cells from ionizing radiation via heme oxygenase-1 (HO-1) overexpression. *J Radiat Res* 2014;55:1056-1065.
20. Katiyar SK, Afaq F, Perez A, Mukhtar H. Green tea polyphenol (-)-epigallocatechin-3-gallate treatment of human skin inhibits ultraviolet radiation-induced oxidative stress. *Carcinogenesis* 2001;22:287-294.
21. Hiipakka RA, Zhang HZ, Dai W, Dai Q, Liao S. Structure-activity relationships for inhibition of human 5alpha-reductases by polyphenols. *Biochem Pharmacol* 2002;63:1165-

- 1176.
22. Kwon OS, Han JH, Yoo HG, Chung JH, Cho KH, Eun HC, et al. Human hair growth enhancement in vitro by green tea epigallocatechin-3-gallate (EGCG). *Phytomedicine* 2007;14: 551-555.
  23. Li Y, Kong D, Wang Z, Sarkar FH. Regulation of microRNAs by natural agents: an emerging field in chemoprevention and chemotherapy research. *Pharm Res* 2010;27:1027-1041.
  24. Kim OY, Cha HJ, Ahn KJ, An IS, An S, Bae S. Identification of microRNAs involved in growth arrest and cell death in hydrogen peroxide-treated human dermal papilla cells. *Mol Med Rep* 2014;10:145-154.
  25. Chung JH, Han JH, Hwang EJ, Seo JY, Cho KH, Kim KH, et al. Dual mechanisms of green tea extract (EGCG)-induced cell survival in human epidermal keratinocytes. *FASEB J* 2003;17:1913-1915.
  26. Zheng Y, Lim EJ, Wang L, Smart EJ, Toborek M, Hennig B. Role of caveolin-1 in EGCG-mediated protection against linoleic-acid-induced endothelial cell activation. *J Nutr Biochem* 2009;20:202-209.
  27. Elbling L, Herbacek I, Weiss RM, Jantschitsch C, Micksche M, Gerner C, et al. Hydrogen peroxide mediates EGCG-induced antioxidant protection in human keratinocytes. *Free Radic Biol Med* 2010;49:1444-1452.
  28. Gu JW, Makey KL, Tucker KB, Chinchar E, Mao X, Pei I, et al. EGCG, a major green tea catechin suppresses breast tumor angiogenesis and growth via inhibiting the activation of HIF-1 $\alpha$  and NF $\kappa$ B, and VEGF expression. *Vasc Cell* 2013;5:9.
  29. Shankar S, Marsh L, Srivastava RK. EGCG inhibits growth of human pancreatic tumors orthotopically implanted in Balb C nude mice through modulation of FKHL1/FOXO3a and neuropilin. *Mol Cell Biochem* 2013;372:83-94.
  30. Fang CY, Wu CC, Hsu HY, Chuang HY, Huang SY, Tsai CH, et al. EGCG inhibits proliferation, invasiveness and tumor growth by up-regulation of adhesion molecules, suppression of gelatinases activity, and induction of apoptosis in nasopharyngeal carcinoma cells. *Int J Mol Sci* 2015;16: 2530-2558.
  31. Ahn WS, Huh SW, Bae SM, Lee IP, Lee JM, Namkoong SE, et al. A major constituent of green tea, EGCG, inhibits the growth of a human cervical cancer cell line, CaSki cells, through apoptosis, G(1) arrest, and regulation of gene expression. *DNA Cell Biol* 2003;22:217-224.
  32. Upton JH, Hannen RF, Bahta AW, Farjo N, Farjo B, Philpott MP. Oxidative stress-associated senescence in dermal papilla cells of men with androgenetic alopecia. *J Invest Dermatol* 2015;135:1244-1252.
  33. Liu S, Navarro G, Mauvais-Jarvis F. Androgen excess produces systemic oxidative stress and predisposes to beta-cell failure in female mice. *PLoS One* 2010;5:e11302.
  34. Lu LY, Ou N, Lu QB. Antioxidant induces DNA damage, cell death and mutagenicity in human lung and skin normal cells. *Sci Rep* 2013;3:3169.
  35. Finkel T. Signal transduction by reactive oxygen species. *J Cell Biol* 2011;194:7-15.
  36. Tsuchiya S, Fujiwara T, Sato F, Shimada Y, Tanaka E, Sakai Y, et al. MicroRNA-210 regulates cancer cell proliferation through targeting fibroblast growth factor receptor-like 1 (FGFR1). *J Biol Chem* 2011;286:420-428.
  37. Yang W, Sun T, Cao J, Liu F, Tian Y, Zhu W. Downregulation of miR-210 expression inhibits proliferation, induces apoptosis and enhances radiosensitivity in hypoxic human hepatoma cells in vitro. *Exp Cell Res* 2012;318:944-954.
  38. Kiga K, Mimuro H, Suzuki M, Shinozaki-Ushiku A, Kobayashi T, Sanada T, et al. Epigenetic silencing of miR-210 increases the proliferation of gastric epithelium during chronic *Helicobacter pylori* infection. *Nat Commun* 2014;5:4497.
  39. Kim JH, Park SG, Song SY, Kim JK, Sung JH. Reactive oxygen species-responsive miR-210 regulates proliferation and migration of adipose-derived stem cells via PTPN2. *Cell Death Dis* 2013;4:e588.
  40. Jiang X, Xiang G, Wang Y, Zhang L, Yang X, Cao L, et al. MicroRNA-590-5p regulates proliferation and invasion in human hepatocellular carcinoma cells by targeting TGF- $\beta$  RII. *Mol Cells* 2012;33:545-551.
  41. Shan X, Miao Y, Fan R, Qian H, Chen P, Liu H, et al. MiR-590-5P inhibits growth of HepG2 cells via decrease of S100A10 expression and Inhibition of the Wnt pathway. *Int J Mol Sci* 2013;14:8556-8569.
  42. Chu Y, Ouyang Y, Wang F, Zheng A, Bai L, Han L, et al. MicroRNA-590 promotes cervical cancer cell growth and invasion by targeting CHL1. *J Cell Biochem* 2014;115: 847-853.
  43. Fan C, Liu S, Zhao Y, Han Y, Yang L, Tao G, et al. Upregulation of miR-370 contributes to the progression of gastric carcinoma via suppression of FOXO1. *Biomed Pharmacother* 2013;67:521-526.
  44. Wu Z, Sun H, Zeng W, He J, Mao X. Upregulation of MicroRNA-370 induces proliferation in human prostate cancer cells by downregulating the transcription factor FOXO1. *PLoS One* 2012;7:e45825.
  45. Wu J, Lv Q, He J, Zhang H, Mei X, Cui K, et al. MicroRNA-188 suppresses G1/S transition by targeting multiple cyclin/CDK complexes. *Cell Commun Signal* 2014;12:66.
  46. Schneider C, Setty M, Holmes AB, Maute RL, Leslie CS, Mussolin L, et al. MicroRNA 28 controls cell proliferation and is down-regulated in B-cell lymphomas. *Proc Natl Acad Sci U S A* 2014;111:8185-8190.